Canadian Science Publishing | Canadian Journal of Physiology and Pharmacology

Cardioprotective effect of fingolimod against calcium paradox-induced myocardial injury in the isolated rat heart

Journal:	*Canadian Journal of Physiology and Pharmacology*
Manuscript ID	cjpp-2021-0381.R2
Manuscript Type:	Article
Date Submitted by the Author:	08-Sep-2021
Complete List of Authors:	Alatrag, Fatma; University of Cape Town, Human Biology Amoni, Matthew; University of Cape Town, Human Biology Kelly-Laubscher, Roisin; University of Cape Town, Biological Sciences; University College Cork, Department of Pharmacology and Therapeutics Gwanyanya, Asfree; University of Cape Town, Human Biology
Is the invited manuscript for consideration in a Special Issue:	Not applicable (regular submission)
Keyword:	cardiac, calcium paradox, fingolimod, ion channels, TRPM7

Cardioprotective effect of fingolimod against calcium paradox-induced myocardial injury in the isolated rat heart

Fatma Alatrag, Matthew Amoni, Roisin Kelly-Laubscher, and Asfree Gwanyanya

F. Alatrag., M. Amoni., and A. Gwanyanya. Department of Human Biology, Faculty of Health Sciences, University of Cape Town, Observatory 7925, Cape Town, South Africa.

R. Kelly-Laubscher. Department of Pharmacology and Therapeutics, The College of Medicine and Health, University College Cork, Ireland.

R. Kelly-Laubscher. Department of Biological Sciences, Faculty of Science, University of Cape Town, Rondebosch 7700, Cape Town, South Africa.

Corresponding author: Asfree Gwanyanya.

Department of Human Biology, Faculty of Health Sciences, University of Cape Town, Observatory 7925, Cape Town, South Africa. Tel: +27216506400; Fax: +27214487226

E-mail: asfree.gwanyanya@uct.ac.za

Abstract: Fingolimod (FTY720) inhibits Ca^{2+}-permeable, Mg^{2+}-sensitive channels called transient receptor potential melastatin 7 (TRPM7), but its effects on Ca^{2+} paradox (CP)-induced myocardial damage have not been evaluated. We studied the effect of FTY720 on CP-induced myocardial damage, and used other TRPM7 channel inhibitors nordihydroguaiaretic acid (NDGA) and Mg^{2+} to test if any effect of FTY720 was via TRPM7 inhibition. Langendorff-perfused Wistar rat hearts were treated with FTY720 or NDGA and subjected to a CP protocol consisting of Ca^{2+} depletion followed by Ca^{2+} repletion. Hearts of rats pre-treated with $MgSO_4$ were also subjected to CP. Hemodynamic parameters were measured using an intraventricular balloon, and myocardial infarct size was quantified using triphenyltetrazolium chloride stain. TRPM7 proteins in ventricular tissue were detected using immunoblot analysis. FTY720, but not NDGA, decreased CP-induced infarct size. Both FTY720 and NDGA minimized the CP-induced elevation of left ventricular end-diastolic pressure, but only FTY720 ultimately improved ventricular developed pressure. Mg^{2+} pre-treatment had effect neither on CP-induced infarct size, hemodynamic parameters during CP, nor the level TRPM7 protein expression in ventricular tissue. Overall, FTY720 attenuated CP-induced myocardial damage, with potential therapeutic implications on Ca^{2+}-mediated cardiotoxicity. However, the cardioprotective mechanism of FTY720 seems to be unrelated to TRPM7 channel modulation.

Keywords

cardiac; calcium paradox; fingolimod; ion channels; TRPM7

Introduction

Abnormalities of calcium (Ca^{2+}) homeostasis underlie the pathophysiology of life-threatening cardiovascular conditions such as myocardial injury and malignant arrhythmias (Wagner et al. 2015). Ca^{2+} paradox (CP) is a form of Ca^{2+}-mediated myocardial injury that may occur perioperatively in hearts temporarily subjected to Ca^{2+}-deficient conditions such as perfusion with Ca^{2+}-free cardioplegic solutions (Zimmerman 2000). In other non-perioperative situations, cardiac Ca^{2+} paradox could occur in a subtle form and remain relatively undetected in conditions of temporary Ca^{2+} deficits. Unlike the myocardium damage due to ischemia/reperfusion injury, CP can occur even with continuous tissue perfusion (Mani et al. 2015, Piper 2000). During CP, the removal of extracellular Ca^{2+} induces cardiac intracellular- and intercellular molecular changes that make cardiomyocytes susceptible to damage upon the re-introduction of extracellular Ca^{2+} ions (Aggeli et al. 2013, Hearse et al. 1978, Zimmerman 2000). Unfortunately, preventative options for CP remain limited because the underlying mechanisms are not fully understood. The known abnormalities in CP include myocardial ultra-structural damage mainly due to Ca^{2+} overload as well as due to cell-cell separation and ATP depletion, even in the absence of ischemia (Kovacs et al. 2017, Mani et al. 2015, Piper 2000). The Ca^{2+} overload in CP may occur via Ca^{2+}-selective channels such as L-type Ca^{2+} channels or secondary to Na^{+} overload via the action of the reverse-mode Na^{+}/Ca^{2+} exchanger (Guppy et al. 1999, Karmazyn et al. 1993, Piper 2000). It has also been suggested to occur via Ca^{2+}-permeable channels such as transient receptor potential (TRP) channels (Bosteels et al. 1999, Kojima et al. 2010).

Fingolimod (FTY720) is a drug used in the treatment of multiple sclerosis, but some studies have also demonstrated its ability to protect against cardiovascular conditions such as ischemia/reperfusion myocardial injury (Hofmann et al. 2009, Santos-Gallego et al. 2016, Vessey et al. 2013) and arrhythmias (Egom et al. 2010, Egom et al. 2015). Nonetheless, even

in the context of ischemia/reperfusion injury, the effect of FTY720 is still not fully known since both pro-arrhythmic and anti-arrhythmic effects of FTY720 have been observed in the same disease model, depending on the timing of drug administration (Hofmann et al. 2010). Furthermore, in ischemia/reperfusion injury models, FTY720 has been shown either to reduce infarct size (van Vuuren et al. 2016), to have no effect on infarct size, despite hemodynamic improvements (Hofmann et al. 2009, Hofmann et al. 2010), or to have a dose-dependent differential effect on functional recovery (van Vuuren et al. 2016).

The pathophysiological mechanisms of disease conditions such as ischemia/reperfusion myocardial injury are distinctly different from that of CP (Piper 2000), and as such the effect of FTY720 on CP-induced myocardial damage is unknown. FTY720 is a sphingosine analogue. When protecting the heart against damage caused by ischemia/reperfusion injury or arrhythmias, FTY720 has been shown to act through S1P receptor-dependent mechanisms and activation of pro-survival kinases to protect the heart (Ahmed et al. 2019, Egom et al. 2010, Hofmann et al. 2009, Hofmann et al. 2010, Santos-Gallego et al. 2016). Interestingly, FTY720 also acts via S1P receptor-independent pathways to protect the heart (Vessey et al. 2013). One of these mechanisms is via its inhibition of the enzyme S1P lyase (Bandhuvula et al. 2005), the inhibition of which is linked to the cardioprotection against ischemia/reperfusion injury (Bandhuvula et al. 2011). However, FTY720 can also inhibit the Mg^{2+}-sensitive, Ca^{2+}-permeable TRP melastatin 7 (TRPM7) channels (Qin et al. 2013). The TRPM7 channels mediate cellular entry of Ca^{2+} and other divalent cations (Gwanyanya et al. 2004, Monteilh-Zoller et al. 2003, Nadler et al. 2001). Considering the major changes in Ca^{2+} homeostasis that occur in several cardiac pathologies, it is possible that FTY720 may also protect the heart via its modulation of these channels.

In this study, we therefore investigated the effect of FTY720 on CP-induced myocardial damage. We also tested whether FTY720 may act via inhibiting TRPM7 channels

by using another chemically-unrelated TRPM7 inhibitor nordihydroguaiaretic acid (NDGA) (Chen et al. 2010) as well as Mg^{2+}, given its intracellular inhibition of TRPM7 channels (Gwanyanya et al. 2004, Monteilh-Zoller et al. 2003). TRPM7 channels were targeted because they are a relatively new type of Ca^{2+}-permeable channels that are known to be inhibited by fingolimod, and therefore can become therapeutic drug targets. As for Mg^{2+}, its extracellular application is already known to protect against Ca^{2+} paradox in guinea pig hearts (Suleiman et al. 1993), so we tested for a different, intracellular effect of Mg^{2+} on CP via TRPM7 inhibition.

Materials and methods

Animals

The study was approved by the Faculty of Health Sciences Animal Research Ethics Committee of the University of Cape Town (AEC Protocol 014-014), and all research involving animals was conducted according to the Canadian Council on Animal Care (CCAC) guidelines and the Guide for the Care and Use of Laboratory Animals (8th edition, National Academies Press). Adult male Wistar rats (250–300 g) were housed under standardized conditions (12-hour light/dark cycle and temperature of 23°C) and had unlimited access to rat chow and drinking water. Rats used to test Mg^{2+} effects were injected intraperitoneally (i.p.) with either $MgSO_4$ (270 mg/kg) or an equivalent volume of saline daily for 7 consecutive days (Amoni et al. 2017b, Sameshima et al. 1999). The $MgSO_4$ salt was chosen as it is more often clinically used than say $MgCl_2$ (Durlach et al. 2005), and also offsets any enteral-route related toxicity when administered intraperitoneally as was done in this study. For enteral administration, $MgCl_2$ would have been a better choice, given its lower enteral toxicity profile (Durlach et al. 2005). In addition, the $MgSO_4$ pharmacokinetic profile in rats has been determined in other tissue-protection studies (Sameshima et al. 1999). Mg^{2+} was administered as pre-treatment in vivo, rather than acutely on isolated hearts in order to allow the Mg^{2+} to enter cells and exert its TRPM7 channel inhibitory effects from the intracellular compartment (Gwanyanya et al. 2004, Monteilh-Zoller et al. 2003, Nadler et al. 2001). The experiments on Mg^{2+}-treated rats were performed 24 hours after the final $MgSO_4$ or saline injection to exclude direct extracellular effects of Mg^{2+}.

Heart isolation and perfusion protocols

Unless stated otherwise, chemicals were obtained from Sigma (Sigma-Aldrich, SA). Hearts were removed for Langendorff perfusion as previously described (Araibi et al. 2020). Briefly, rats were anticoagulated with heparin (500 I.U./kg, i.p.) and anesthetized with sodium pentobarbital (70 mg/kg i.p., Vertserv, SA). Hearts were rapidly removed and placed in cold (4°C), filtered (Whatman filter paper, Sigma-Aldrich, SA), modified Krebs-Henseleit (K-H) solution containing (in mmol/L): 118.5 NaCl, 4.7 KCl, 25 $NaHCO_3$, 1.2 $MgSO_4$, 1.8 $CaCl_2$, 1.2 KH_2PO_4 and 11 glucose; pH 7.4, gassed with 95%O_2 and 5%CO_2). For perfusion studies, the aorta was cannulated for retrograde perfusion with K-H solution (maintained at 37°C) on a constant-pressure (74 mmHg) Langendorff perfusion apparatus (Fig. 1A). To induce Ca^{2+} paradox, a parallel Langendorff apparatus was used to deliver Ca^{2+}-free K-H solution, and this system converged with the main perfusion system via a 3-way stop cock positioned above the aortic cannula (Fig. 1A). The Ca^{2+}-free K-H solution was made by excluding $CaCl_2$ from K-H solution and adding 0.5 mmol/L EGTA.

Hearts used to test the effects of fingolimod (FTY720) and NDGA were randomly assigned to 6 groups (Fig. 1B), whereas those used to test the effect of Mg^{2+} were assigned to 4 groups (Fig. 4A), with each group named according to the perfusion- and drug administration protocol used. Hearts were stabilized on the perfusion system for 20 minutes prior to drug treatments. The CP protocol consisted of heart perfusion with Ca^{2+}-free K-H solution for 3 minutes, followed by the re-introduction of Ca^{2+}-containing solution for 30 minutes (Bi et al. 2012). FTY720 (1 µmol/L) and NDGA (10 µmol/L) were dissolved in DMSO (final concentration < 0.01%) and administered for 5 minutes before the commencement of the CP protocol. The concentrations of these drugs used are adequate to inhibit TRPM7 channels (Chen et al. 2010, Qin et al. 2013). The drugs were delivered into the perfusate column through a 3-way stop cock using a syringe pump (Graseby 2100, Smith Medical, SA; Fig 1A) set to run at 10% of the coronary flow rate in order to minimize

disturbances in perfusion pressure. The concentration of the drug in the syringe was 10 times higher than the final concentration to cater for the dilution by the main perfusion column. The coronary flow rate was measured by timed collection of coronary effluent. At the end of perfusion, hearts were stored at -20°C for infarct size measurements.

Hemodynamic parameter measurements

Left ventricular (LV) pressure was measured using a water-filled, intraventricular balloon (Fig. 1A) mounted at the tip of a catheter connected to a blood pressure transducer (MLT1199) and amplifier (Bridge Amp ML221, ADInstruments, Australia). The balloon was inflated to a LV end-diastolic pressure (LVEDP) of 5−10 mmHg, and the balloon volume was not altered thereafter. Hemodynamic parameters were recorded using the PowerLab data-acquisition system and LabChart 7 software (ADInstruments, Australia) and were analyzed using the LabChart 7 Pro BP module (ADInstruments, Australia). The LV developed pressure (LVDP) was obtained as the difference between peak systolic pressure and LVEDP.

Infarct size measurements

Ventricles of frozen hearts were cut transversely into a series of 2-mm slices from apex to base and thawed for 2,3,5-triphenyltetrazolium chloride (TTC) staining as previously described (Amoni et al. 2017b, Araibi et al. 2020). Infarct size was measured as TTC-negative area on the slices from each heart using ImageJ software (NIH, USA) and was expressed as a percentage of the total ventricular area (Araibi et al. 2020).

Western immunoblotting

Western blot analysis was performed as previously described (Aboalgasm et al. 2021a, Aboalgasm et al. 2021b). Sections of frozen LV tissue (approximately 0.05 g) were

homogenized on ice by sonication in a modified radioimmunoprecipitation assay (RIPA) lysis buffer (50 mM Tris-HCl, 150 mM NaCl, 1% Triton X-100, 0.5% sodium deoxycholate, 0.1% sodium dodecyl sulphate, pH 7.4) containing a protease/phosphatase inhibitor cocktail (HALT, Thermo Fisher Scientific, Rockford, USA). The samples were mixed on a vortex and centrifuged at 15 000 g for 30 minutes at 4°C. The supernatant was decanted, and the protein concentration was quantified using a BCA protein assay kit (Thermo Fisher Scientific, Rockford, USA). Lysates were denatured at 95°C for 5 minutes in a mixture of Laemmli buffer (Bio-Rad, SA), RIPA buffer, and diethyltritriol. Protein samples (40 µg) were electrophoresed on 12% SDS-PAGE gels using a Mini-PROTEAN Tetra Cell system (Bio-Rad, SA) and transferred to nitrocellulose membrane using a Trans-Blot turbo transfer system (Bio-Rad, SA). Gel electrophoresis and protein transfer to membrane were confirmed by Ponceau S staining. The membrane was blocked with 5% milk in 0.1% Tween-20 phosphate-buffered saline (PBS-T) at 4°C for 3 hours, and incubated with anti-TRPM7 mouse monoclonal primary antibody (1:8000, Abcam 85016, USA) in 5% milk PBS-T overnight at 4°C. In the negative control, anti-TRPM7 antibody was excluded to rule out non-specific binding of secondary antibody. The membrane was then washed in PBS-T and incubated with horseradish peroxidase-linked goat anti-mouse secondary antibody (1:20 000, Abcam 205719, USA) in 5% milk PBS-T for 1 hour at room temperature. Blots were developed by adding an enhanced chemiluminescence substrate (Bio-Rad, SA) and exposure to X-ray film. The film images were scanned and analysed using ImageJ software (NIH, USA). The membrane was thereafter washed in water, stripped with 8% NaOH, blocked for 3 hours with 5% BSA in PBS-T, and re-probed with anti-β-actin mouse monoclonal primary antibody (1:15000, Abcam 8226, USA) and goat anti-mouse secondary antibody (1:20 000, Abcam 205719, USA).

196 **Plasma Mg^{2+} measurements**

197 Blood used for Mg^{2+} measurements was collected at the time of excision of the heart
198 (24 hours after the final $MgSO_4$ or saline injection). The blood was centrifuged to obtain
199 plasma, from which ionized Mg^{2+} concentration was measured using photometric assays
200 (Beckman AU, PathCare, SA) as previously described (Amoni et al. 2017a).
201

202 **Data analysis**

203 Data are expressed as mean and standard error of mean (SEM), with *n* indicating the
204 number of rats studied under each condition. Statistical analysis was conducted using
205 Statistica (v.13). Differences among multiple groups were evaluated using analysis of
206 variance (ANOVA) and Tukey's *post-hoc* test or repeated-measures ANOVA. Differences
207 between two independent groups were compared using unpaired *t*-test. $P < 0.05$ was
208 considered statistically significant.

Results

Effects of FTY720 and NDGA on CP-induced infarct size

Representative images of TTC-stained ventricular slices (Fig. 2A) show a prominent TTC-negative ventricular area in the CP heart compared to that in the control heart, which is indicative of CP-induced myocardial damage. The application of FTY720 (1 μmol/L), but not NDGA (10 μmol/L), significantly decreased CP-induced infarct size from 64.6 ± 5.3% to 39.0 ± 6.8% ($P = 0.001$; Fig. 2B). The sizes of background infarcts due to handling artefacts in non-CP hearts (i.e., control and drug only treated hearts) were not significantly different from each other ($P = 0.78$) but were significantly smaller than the infarcts in CP hearts ($P < 0.001$; Fig. 2B).

Effects of FTY720 and NDGA on CP-induced hemodynamic parameters

A typical CP protocol (Fig. 3A) produced a complete loss of ventricular force of contraction and an elevation of LVEDP during the periods of Ca^{2+} depletion and Ca^{2+} repletion (LVEDP: $P < 0.001$ for CP vs. control; Fig. 3B), whereas the ventricular force of contraction and LVEDP in control, non-CP hearts remained relatively stable over the duration of perfusion. Although there was still an elevation of LVEDP due to CP, both FTY720 and NDGA decreased the extent of CP-induced elevation of LVEDP compared to CP alone ($P = 0.039$ for FTY720 + CP vs. CP and $P = 0.020$ for NDGA + CP vs. CP; Fig. 3B). However, only FTY720 significantly improved LVDP during CP ($P = 0.029$, FTY720 + CP vs. CP; Fig. 3C). In the absence of CP, neither FTY720 nor NDGA altered LVDP compared to control ($P = 0.90$; Fig. 3C). However, FTY720 alone increased LVEDP in the absence of CP compared to control ($P = 0.003$), but this increase was still significantly lower than the LVEDP in CP (Fig. 3B). Neither CP nor the application of drugs (FTY720 or

NDGA) had statistically significant effect on coronary flow rate compared to control ($P = 0.40$; Fig. 3D).

Effect of Mg^{2+} on CP

We also tested effects of Mg^{2+} as an additional type of TRPM7 channel inhibitor. This ion has a different inhibitory action since it acts intracellularly as compared to the extracellular effects of FTY720 and NDGA. Mg^{2+} pre-treatment did not significantly alter CP-induced infarct size (50.7 ± 3.7% for CP vs. 50.2 ± 4.1% for Mg^{2+} + CP, $P = 0.98$; Fig. 4B and Fig. 4C). The sizes of background infarcts in non-CP hearts were not significantly different from each other (infarct size: 7.4 ± 0.5% for control vs. 6.4 ± 0.5% for Mg^{2+} pre-treated, $P = 0.90$), but were significantly smaller than the infarcts in CP hearts ($P < 0.001$, CP vs. control or Mg^{2+}; Fig. 4B and Fig. 4C). Mg^{2+} pre-treatment also did not reverse the CP-induced changes in LVEDP or LVDP (Fig. 4D and Fig. 4E). In the absence of CP, pre-treatment with Mg^{2+} had no significant effect on LVDP or LVEDP (Fig. 4D and Fig. 4E). Furthermore, Mg^{2+} concentration was measured to verify plasma normomagnesemia at the time of CP experiments. The plasma Mg^{2+} concentration was not significantly different between Mg^{2+} pre-treated rats and controls (0.87 ± 0.03 mmol/L for control vs. 0.93 ± 0.04 mmol/L for Mg^{2+} pre-treated; $P = 0.62$, n = 5 rats per group).

TRPM7 immunoblotting

In order to verify the presence of TRPM7 channels and the possible modulation by Mg^{2+} pre-treatment in the rat hearts used in our experiments, TRPM7 immunoblotting was performed in ventricular tissue. Images of western blot analysis (Fig. 5A) showed the immune-detection of both TRPM7- and the loading control β-actin proteins in cardiac LV tissue. In contrast, the TRPM7 signal was virtually undetectable in the negative controls in

258 which the anti-TRPM7 primary antibody was omitted (P = 0.003 vs. TRPM7; n = 6 rats per
259 group; result not illustrated). The intensity of the TRPM7 bands on films appeared similar in
260 ventricular tissue of control rats and Mg^{2+} pre-treated rats (Fig. 5A). As such, there was no
261 statistically significant difference in the level of TRPM7 protein expression between
262 ventricular tissue of control- and Mg^{2+} pre-treated rats (P = 0.43; Fig. 5B).

Discussion

CP represents a unique, Ca^{2+}-related threat to perioperative cardiovascular tissue survival, even in the absence of ischemia (Piper 2000, Zimmerman 2000). The results of the present study showed that FTY720, but not NDGA nor Mg^{2+}, decreased CP-induced infarct size and improved LV functional recovery.

In this study, FTY720 was partially effective at rescuing contractile function of the heart during CP as was evidenced by improved LVDP; minimized cardiac tissue death from CP-induced myocardial injury as was evidenced by the reduction in infarct size; and reduced the extent of dysfunctional contractures as was indicated by decreased LVEDP during CP. Although some studies have demonstrated cardioprotective effects of FTY720 in models of ischemia/reperfusion injury and cardiac arrhythmia, this cardioprotective effect of FTY720 during CP seems to be a novel finding since there were no previous reports that we could find that specifically addressed the effect of FTY720 on CP. However, we also noticed that FTY720, on its own, increased LVEDP by the end of perfusion compared to control hearts. The reason for this increase was not clear, but other studies showed that the infusion of FTY720 in conscious rodents increased mean arterial pressure (Forrest et al. 2004), and that FTY720, when orally administered, induced hypertension in rodents (Fryer et al. 2012). In contrast, in healthy human subjects, FTY720 induced transient decreases in mean arterial pressure (Schmouder et al. 2006). Such effects of FTY720 on blood pressure as well as the induction of bradycardia (Faber et al. 2013) therefore constitute important side effects to be recognized in the utility of the drug in cardioprotection. Nonetheless, the increase in LVEDP by FTY720 observed in the present study did not undermine the overall improvement of LVDP during CP.

The mechanism underlying the cardioprotective effect of FTY720 during CP is unclear since the inhibition of TRPM7 channel did not seem to mediate the effect. In our

study, there was a lack of cardioprotection against CP by NDGA, a chemical which, similar to FTY720, inhibits the Ca^{2+}-permeable TRPM7 channels at the doses administered (Chen et al. 2010, Qin et al. 2013). The lack of NDGA effect was despite the presence of TRPM7 protein in the rat hearts used in our experiments as was confirmed by the positive TRPM7 immunoblots in LV tissue. Consistent with the findings from another study (Murphy et al. 1995), in our study, NDGA, on its own, had no detrimental effects on cardiac hemodynamic function, but rather stabilized LVEDP during CP. However, NDGA was also shown to impair protective effects of cardiac preconditioning via the lipoxygenase pathway (Murphy et al. 1995) but such a mechanism may not be relevant to CP since the inhibition of TRPM7 channels by NDGA is lipoxygenase-independent (Chen et al. 2010). Furthermore, in our study, Mg^{2+} pre-treatment did no alter CP, suggesting that the intracellular inhibitory effect of Mg^{2+} on TRPM7 channels did not modulate CP. The protective effect of acute extracellular Mg^{2+} against CP observed in guinea pig hearts (Suleiman et al. 1993) is different from an intracellular inhibition of TRPM7 channels, and therefore would not be applicable in the present study since the plasma Mg^{2+} concentration had reverted to normal at the time of CP experiments as was verified by Mg^{2+} assays. Taken together, our results suggest that the cardioprotective effect of FTY720 during CP may be unrelated to the inhibition of TRPM7 channels. The possible contribution to CP of other TRP channels that belong to the same melastatin subfamily as TRPM7 channels such as TRPM4 is not known. TRPM4 channels are highly selective for monovalent cations such as Na^{+} (Launay et al. 2002), and it has been proposed that the monovalent cation influx through them could induce membrane depolarisation that may, in turn, cause Ca^{2+} influx via Ca^{2+}-permeable channels, thereby modulating cardiac activity (Alonso-Carbajo et al. 2017). However, there is no evidence yet to support this possibility for Ca^{2+} influx through TRPM7 channels, which would otherwise be relevant in CP. In addition, such an effect would most likely affect voltage-gated Ca^{2+}-

permeable channels, rather than TRPM7 channels, for which the gating is voltage-independent (Gwanyanya et al. 2004, Monteilh-Zoller et al. 2003, Nadler et al. 2001).

Most of what is currently known about the cardiac effects of FTY720 relates to the models of ischemia/reperfusion injury. Although Ca^{2+} dysregulation may be involved in both ischemia/reperfusion injury and Ca^{2+} paradox, these conditions are different. Ca^{2+} paradox is not often easily recognised as it presents with some features similar to those of ischemia/reperfusion injury (Hearse et al. 1978), yet it is a detrimental clinical entity that occurs even in the absence of an ischemic insult (Aggeli et al. 2013, Hearse et al. 1978, Zimmerman 2000). Furthermore, given that Ca^{2+} paradox represents a complication of temporary Ca^{2+} deficit, but, at the same time, Ca^{2+} abnormalities are known to affect a plethora of cellular functions, its manifestation could be missed and attributed to other well-known Ca^{2+}-related cellular events. However, an important limitation in studying Ca^{2+} paradox (as was done in the present study) is that the standard experimental protocol of extracellular Ca^{2+} exclusion is extreme and unphysiological, but at the same time, it has the advantage that it amplifies and quickens the subtle tissue damage that would otherwise occur undetected whenever there is a temporary Ca^{2+} deficit (Piper 2000). Our results, therefore, show the potential of FTY720 as a cardioprotective agent against Ca^{2+} paradox, a novelty that has not been described in Ca^{2+} paradox. This FTY720 effect on CP is therefore different from the FTY720 modulation of other cardiac conditions such as ischaemia/reperfusion injury. However, the exact mechanism underlying the protective effect of FTY720 against CP was not established in the present study.

In conclusion, the results of this study showed that FTY720, but not NDGA or Mg^{2+}, partially reduced CP-induced myocardial damage and improved cardiac contractile function. Clinically, given that FTY720 is already being used in the treatment of multiple sclerosis, this cardioprotective effect may represent a novel therapeutic role of the drug (or in combination

with other protective drugs) in attenuating CP-induced myocardial damage during perioperative cardiac perfusion. The results suggest that the cardioprotective action of FTY720 during CP may be unrelated to the inhibition of TRPM7 channels, but the exact underlying mechanism still requires further investigation.

Acknowledgements

This work was supported by the South African Medical Research Council (MRC SIR Grant number 29841) and the National Research Foundation South Africa (NRF Grant numbers 85768 and 91514). **Conflict of interest:** The authors declare no conflict of interest.

References

Aboalgasm, H., Ballo, R., Mkatazo, T. & Gwanyanya, A. 2021a. Hyperglycaemia-Induced Contractile Dysfunction and Apoptosis in Cardiomyocyte-Like Pulsatile Cells Derived from Mouse Embryonic Stem Cells. Cardiovasc Toxicol. **21**(9): 695-709. doi:10.1007/s12012-021-09660-3. PMID:33983555.

Aboalgasm, H., Petersen, M. & Gwanyanya, A. 2021b. Improvement of cardiac ventricular function by magnesium treatment in chronic streptozotocin-induced diabetic rat heart. Cardiovasc J Afr. **32**(3): 141-148. doi:10.5830/CVJA-2020-054. PMID:33300932.

Aggeli, I.K., Zacharias, T., Papapavlou, G., Gaitanaki, C. & Beis, I. 2013. Calcium paradox induces apoptosis in the isolated perfused Rana ridibunda heart: involvement of p38-MAPK and calpain. Can J Physiol Pharmacol. **91**(12): 1095-1106. doi:10.1139/cjpp-2013-0081. PMID:24289081.

Ahmed, N., Mehmood, A., Linardi, D., Sadiq, S., Tessari, M., Meo, S.A., Rehman, R., Hajjar, W.M., et al. 2019. Cardioprotective Effects of Sphingosine-1-Phosphate Receptor Immunomodulator FTY720 in a Clinically Relevant Model of Cardioplegic Arrest and Cardiopulmonary Bypass. Front. Pharmacol. **10**: 802. doi:10.3389/fphar.2019.00802. PMID:31379576.

Alonso-Carbajo, L., Kecskes, M., Jacobs, G., Pironet, A., Syam, N., Talavera, K. & Vennekens, R. 2017. Muscling in on TRP channels in vascular smooth muscle cells and cardiomyocytes. Cell Calcium. **66**: 48-61. doi:10.1016/j.ceca.2017.06.004. PMID:28807149.

Amoni, M., Kelly-Laubscher, R., Blackhurst, D. & Gwanyanya, A. 2017a. Beneficial Effects of Magnesium Treatment on Heart Rate Variability and Cardiac Ventricular Function in Diabetic Rats. J Cardiovasc Pharmacol Ther. **22**(2): 169-178. doi:10.1177/1074248416653831. PMID:27276916.

Amoni, M., Kelly-Laubscher, R., Petersen, M. & Gwanyanya, A. 2017b. Cardioprotective and Anti-arrhythmic Effects of Magnesium Pretreatment Against Ischaemia/Reperfusion Injury in Isoprenaline-Induced Hypertrophic Rat Heart. Cardiovasc Toxicol. **17**(1): 49-57. doi:10.1007/s12012-015-9355-6. PMID:26696240.

Araibi, H., Van Der Merwe, E., Gwanyanya, A. & Kelly-Laubscher, R. 2020. The effect of sphingosine-1-phosphate on the endothelial glycocalyx during ischemia-reperfusion injury in the isolated rat heart. Microcirculation. **27**(5): e12612. doi:10.1111/micc.12612. PMID:32017300.

Bandhuvula, P., Honbo, N., Wang, G.Y., Jin, Z.Q., Fyrst, H., Zhang, M., Borowsky, A.D., Dillard, L., et al. 2011. S1P lyase: a novel therapeutic target for ischemia-reperfusion injury of the heart. Am J Physiol Heart Circ Physiol. **300**(5): H1753-1761. doi:10.1152/ajpheart.00946.2010. PMID:21335477.

Bandhuvula, P., Tam, Y.Y., Oskouian, B. & Saba, J.D. 2005. The immune modulator FTY720 inhibits sphingosine-1-phosphate lyase activity. J. Biol. Chem. **280**(40): 33697-33700. doi:10.1074/jbc.C500294200. PMID:16118221.

Bi, S.H., Jin, Z.X., Zhang, J.Y., Chen, T., Zhang, S.L., Yang, Y., Duan, W.X., Yi, D.H., et al. 2012. Calpain inhibitor MDL 28170 protects against the Ca^{2+} paradox in rat hearts. Clin Exp Pharmacol Physiol. **39**(4): 385-392. doi:10.1111/j.1440-1681.2012.05683.x. PMID:22356295.

Bosteels, S., Matejovic, P., Flameng, W. & Mubagwa, K. 1999. Sodium influx via a non-selective pathway activated by the removal of extracellular divalent cations: possible role in the calcium paradox. Cardiovasc Res. **43**(2): 417-425. doi:10.1016/s0008-6363(99)00098-x. PMID:10536672.

Chen, H.C., Xie, J., Zhang, Z., Su, L.T., Yue, L. & Runnels, L.W. 2010. Blockade of TRPM7 channel activity and cell death by inhibitors of 5-lipoxygenase. PLoS One. **5**(6): e11161. doi:10.1371/journal.pone.0011161. PMID:20567598.

Durlach, J., Guiet-Bara, A., Pages, N., Bac, P. & Bara, M. 2005. Magnesium chloride or magnesium sulfate: a genuine question. Magnes. Res. **18**(3): 187-192. PMID:16259379.

Egom, E.E., Ke, Y., Musa, H., Mohamed, T.M., Wang, T., Cartwright, E., Solaro, R.J. & Lei, M. 2010. FTY720 prevents ischemia/reperfusion injury-associated arrhythmias in an ex vivo rat heart model via activation of Pak1/Akt signaling. J. Mol. Cell. Cardiol. **48**(2): 406-414. doi:10.1016/j.yjmcc.2009.10.009. PMID:19852968.

Egom, E.E., Kruzliak, P., Rotrekl, V. & Lei, M. 2015. The effect of the sphingosine-1-phosphate analogue FTY720 on atrioventricular nodal tissue. J Cell Mol Med. **19**(7): 1729-1734. doi:10.1111/jcmm.12549. PMID:25864579.

Faber, H., Fischer, H.J. & Weber, F. 2013. Prolonged and symptomatic bradycardia following a single dose of fingolimod. Mult. Scler. **19**(1): 126-128. doi:10.1177/1352458512447596. PMID:22729989.

Forrest, M., Sun, S.Y., Hajdu, R., Bergstrom, J., Card, D., Doherty, G., Hale, J., Keohane, C., et al. 2004. Immune cell regulation and cardiovascular effects of sphingosine 1-phosphate receptor agonists in rodents are mediated via distinct receptor subtypes. J Pharmacol Exp Ther. **309**(2): 758-768. doi:10.1124/jpet.103.062828. PMID:14747617.

Fryer, R.M., Muthukumarana, A., Harrison, P.C., Nodop Mazurek, S., Chen, R.R., Harrington, K.E., Dinallo, R.M., Horan, J.C., et al. 2012. The clinically-tested S1P receptor agonists, FTY720 and BAF312, demonstrate subtype-specific bradycardia (S1P(1)) and hypertension (S1P(3)) in rat. PLoS One. **7**(12): e52985. doi:10.1371/journal.pone.0052985. PMID:23285242.

Guppy, L.J. & Littleton, J.M. 1999. Damaging effects of the calcium paradox are reduced in isolated hearts from ethanol-dependent rats: paradoxic effects of dihydropyridine drugs. J. Cardiovasc. Pharmacol. **34**(6): 765-771. doi:10.1097/00005344-199912000-00001. PMID:10598118.

Gwanyanya, A., Amuzescu, B., Zakharov, S.I., Macianskiene, R., Sipido, K.R., Bolotina, V.M., Vereecke, J. & Mubagwa, K. 2004. Magnesium-inhibited, TRPM6/7-like channel in cardiac myocytes: permeation of divalent cations and pH-mediated regulation. J Physiol. **559**(Pt 3): 761-776. doi:10.1113/jphysiol.2004.067637. PMID:15272039.

Hearse, D.J., Humphrey, S.M., Boink, A.B. & Ruigrok, T.J. 1978. The calcium paradox: metabolic, electrophysiological, contractile and ultrastructural characteristics in four species. Eur. J. Cardiol. **7**(4): 241-256. PMID:689059.

Hofmann, U., Burkard, N., Vogt, C., Thoma, A., Frantz, S., Ertl, G., Ritter, O. & Bonz, A. 2009. Protective effects of sphingosine-1-phosphate receptor agonist treatment after myocardial ischaemia-reperfusion. Cardiovasc Res. **83**(2): 285-293. doi:10.1093/cvr/cvp137. PMID:19416991.

Hofmann, U., Hu, K., Walter, F., Burkard, N., Ertl, G., Bauersachs, J., Ritter, O., Frantz, S., et al. 2010. Pharmacological pre- and post-conditioning with the sphingosine-1-phosphate receptor modulator FTY720 after myocardial ischaemia-reperfusion. Br J Pharmacol. **160**(5): 1243-1251. doi:10.1111/j.1476-5381.2010.00767.x. PMID:20590616.

Karmazyn, M., Ray, M. & Haist, J.V. 1993. Comparative effects of Na^+/H^+ exchange inhibitors against cardiac injury produced by ischemia/reperfusion, hypoxia/reoxygenation, and the calcium paradox. J. Cardiovasc. Pharmacol. **21**(1): 172-178. doi:10.1097/00005344-199301000-00025. PMID:7678674.

Kojima, A., Kitagawa, H., Omatsu-Kanbe, M., Matsuura, H. & Nosaka, S. 2010. Ca^{2+} paradox injury mediated through TRPC channels in mouse ventricular myocytes. Br J Pharmacol. **161**(8): 1734-1750. doi:10.1111/j.1476-5381.2010.00986.x. PMID:20718730.

Kovacs, A., Kalasz, J., Pasztor, E.T., Toth, A., Papp, Z., Dhalla, N.S. & Barta, J. 2017. Myosin heavy chain and cardiac troponin T damage is associated with impaired myofibrillar ATPase activity contributing to sarcomeric dysfunction in Ca^{2+}-paradox rat hearts. Mol Cell Biochem. **430**(1-2): 57-68. doi:10.1007/s11010-017-2954-8. PMID:28213770.

Launay, P., Fleig, A., Perraud, A.L., Scharenberg, A.M., Penner, R. & Kinet, J.P. 2002. TRPM4 is a Ca^{2+}-activated nonselective cation channel mediating cell membrane depolarization. Cell. **109**(3): 397-407. doi:10.1016/s0092-8674(02)00719-5. PMID:12015988.

Mani, H., Tanaka, H., Adachi, T., Ikegawa, M., Dai, P., Fujita, N. & Takamatsu, T. 2015. How Does the Ca^{2+}-paradox Injury Induce Contracture in the Heart? - A Combined Study of the Intracellular Ca^{2+} Dynamics and Cell Structures in Perfused Rat Hearts. Acta Histochem. Cytochem. **48**(1): 1-8. doi:10.1267/ahc.14059. PMID:25861132.

Monteilh-Zoller, M.K., Hermosura, M.C., Nadler, M.J., Scharenberg, A.M., Penner, R. & Fleig, A. 2003. TRPM7 provides an ion channel mechanism for cellular entry of trace metal ions. J. Gen. Physiol. **121**(1): 49-60. doi:10.1085/jgp.20028740. PMID:12508053.

Murphy, E., Glasgow, W., Fralix, T. & Steenbergen, C. 1995. Role of lipoxygenase metabolites in ischemic preconditioning. Circ Res. **76**(3): 457-467. doi:10.1161/01.res.76.3.457. PMID:7859391.

Nadler, M.J., Hermosura, M.C., Inabe, K., Perraud, A.L., Zhu, Q., Stokes, A.J., Kurosaki, T., Kinet, J.P., et al. 2001. LTRPC7 is a Mg.ATP-regulated divalent cation channel required for cell viability. Nature. **411**(6837): 590-595. doi:10.1038/35079092. PMID:11385574.

Piper, H.M. 2000. The calcium paradox revisited: an artefact of great heuristic value. Cardiovasc Res. **45**(1): 123-127. doi:10.1016/s0008-6363(99)00304-1. PMID:10728324.

Qin, X., Yue, Z., Sun, B., Yang, W., Xie, J., Ni, E., Feng, Y., Mahmood, R., et al. 2013. Sphingosine and FTY720 are potent inhibitors of the transient receptor potential melastatin 7 (TRPM7) channels. Br J Pharmacol. **168**(6): 1294-1312. doi:10.1111/bph.12012. PMID:23145923.

Sameshima, H., Ota, A. & Ikenoue, T. 1999. Pretreatment with magnesium sulfate protects against hypoxic-ischemic brain injury but postasphyxial treatment worsens brain damage in seven-day-old rats. Am. J. Obstet. Gynecol. **180**(3 Pt 1): 725-730. doi:10.1016/s0002-9378(99)70279-6. PMID:10076154.

Santos-Gallego, C.G., Vahl, T.P., Goliasch, G., Picatoste, B., Arias, T., Ishikawa, K., Njerve, I.U., Sanz, J., et al. 2016. Sphingosine-1-Phosphate Receptor Agonist Fingolimod Increases Myocardial Salvage and Decreases Adverse Postinfarction Left Ventricular Remodeling in a Porcine Model of Ischemia/Reperfusion. Circulation. **133**(10): 954-966. doi:10.1161/CIRCULATIONAHA.115.012427. PMID:26826180.

Schmouder, R., Serra, D., Wang, Y., Kovarik, J.M., Dimarco, J., Hunt, T.L. & Bastien, M.C. 2006. FTY720: placebo-controlled study of the effect on cardiac rate and rhythm in healthy subjects. J. Clin. Pharmacol. **46**(8): 895-904. doi:10.1177/0091270006289853. PMID:16855074.

Suleiman, M.S. & Chapman, R.A. 1993. Calcium paradox in newborn and adult guinea-pig hearts: changes in intracellular taurine and the effects of extracellular magnesium. Exp. Physiol. **78**(4): 503-516. doi:10.1113/expphysiol.1993.sp003702. PMID:8398104.

Van Vuuren, D., Marais, E., Genade, S. & Lochner, A. 2016. The differential effects of FTY720 on functional recovery and infarct size following myocardial ischaemia/reperfusion. Cardiovasc J Afr. **27**(6): 375-386. doi:10.5830/CVJA-2016-039. PMID:27966000.

Vessey, D.A., Li, L., Imhof, I., Honbo, N. & Karliner, J.S. 2013. FTY720 postconditions isolated perfused heart by a mechanism independent of sphingosine kinase 2 and different from S1P or ischemic postconditioning. Med Sci Monit Basic Res. **19**: 126-132. doi:10.12659/MSMBR.883877. PMID:23567658.

Wagner, S., Maier, L.S. & Bers, D.M. 2015. Role of sodium and calcium dysregulation in tachyarrhythmias in sudden cardiac death. Circ Res. **116**(12): 1956-1970. doi:10.1161/CIRCRESAHA.116.304678. PMID:26044250.

Zimmerman, A.N. 2000. The calcium paradox. Cardiovasc Res. **45**(1): 119-121. doi:10.1016/s0008-6363(99)00323-5. PMID:10728322.

Legends to figures

Fig. 1. Heart perfusion set up and experimental groups. Schematic diagram of the perfusion apparatus and drug administration set up (A). Experimental groups as determined by the cardiac perfusion protocols (B). Each drug, nordihydroguaiaretic acid (NDGA), FTY720 or vehicle (DMSO) was administered at steady-state, after a period of stabilization. Abbreviation: CP, Ca^{2+} paradox.

Fig. 2. Effects of NDGA and FTY720 on Ca^{2+} paradox-induced infarcts. Representative images of 2,3,5-triphenyltetrazolium chloride (TTC) stained mid-ventricular slices of hearts subjected to various drug treatment- and perfusion protocols (A). Viable myocardium appears darker (TTC-positive) compared to the myocardium with irreversible infarcts that appears pale (TTC-negative). Infarct size, expressed as % of total the ventricular area (B). Values are presented as mean ± SEM; n = 6 rats per group; ***$P < 0.001$ vs. control; **$P = 0.003$ vs. control; $^{\#\#}P = 0.001$ vs. CP. Abbreviations: FTY, FTY720; CP, Ca^{2+} paradox.

Fig. 3. Effects of NDGA and FTY720 on Ca^{2+} paradox-induced hemodynamic changes. Screenshot images of typical left ventricular (LV) pressure recordings in control- and Ca^{2+} paradox hearts (A). Summary data of LV end-diastolic pressure (LVEDP), LV developed pressure (LVDP), and coronary flow rate (B-D). The parameters were measured at the beginning (baseline) and at the end of the perfusion protocols from different hearts [○, control; ●, Ca^{2+} paradox (CP); □, nordihydroguaiaretic acid (NDGA); ■, NDGA + CP; Δ, FTY720 (FTY); ▲, FTY720 + CP]. Values are presented as mean ± SEM; n = 6 rats per group; ***$P < 0.001$ for CP vs. control; **$P = 0.008$ for FTY720 + CP vs. control or $P = 0.006$ for NDGA + CP vs. control; $^{\#}P = 0.039$ for FTY720 + CP vs. CP or $P = 0.020$ for

NDGA + CP vs. CP; §$P = 0.029$ for FTY720 + CP vs. CP; n.s., not statistically significant ($P = 0.40$).

Fig. 4. Effect of Mg^{2+} pre-treatment on Ca^{2+} paradox. Experimental groups as determined by the type of pre-treatment and cardiac perfusion protocols (A). Abbreviations: Mg, Mg^{2+}; i.p., intraperitoneal; CP, Ca^{2+} paradox. Representative images of TTC-stained mid-ventricular slices of hearts from different experimental protocols (B). Infarct size, expressed as % of the ventricular area (C). Left ventricular (LV) hemodynamic parameters [LV end-diastolic pressure (LVEDP) and LV developed pressure (LVDP)] measured at baseline and at the end of the perfusion protocol in the various groups of hearts [○, control; □, Mg^{2+}; ●, CP; ■, Mg^{2+} + CP] (D-E). Values are presented as mean ± SEM; n ≥ 6 rats per group; ***$P < 0.001$ for Mg + CP or CP vs. control; **$P = 0.001$ for Mg + CP vs. control.

Fig. 5. TRPM7 protein expression in ventricular tissue. Representative Western blot film images of TRPM7 and β-actin in left ventricular tissue of control (untreated) rats and Mg^{2+}-pre-retreated rats (A). Summary data of TRPM7 protein expression, relative to that of β-actin (B). Values are presented as mean ± SEM; n = 6 rats per group; n.s., not statistically significant ($P = 0.43$). Abbreviation: TRPM7, transient receptor potential melastatin 7.

FIGURE 1.

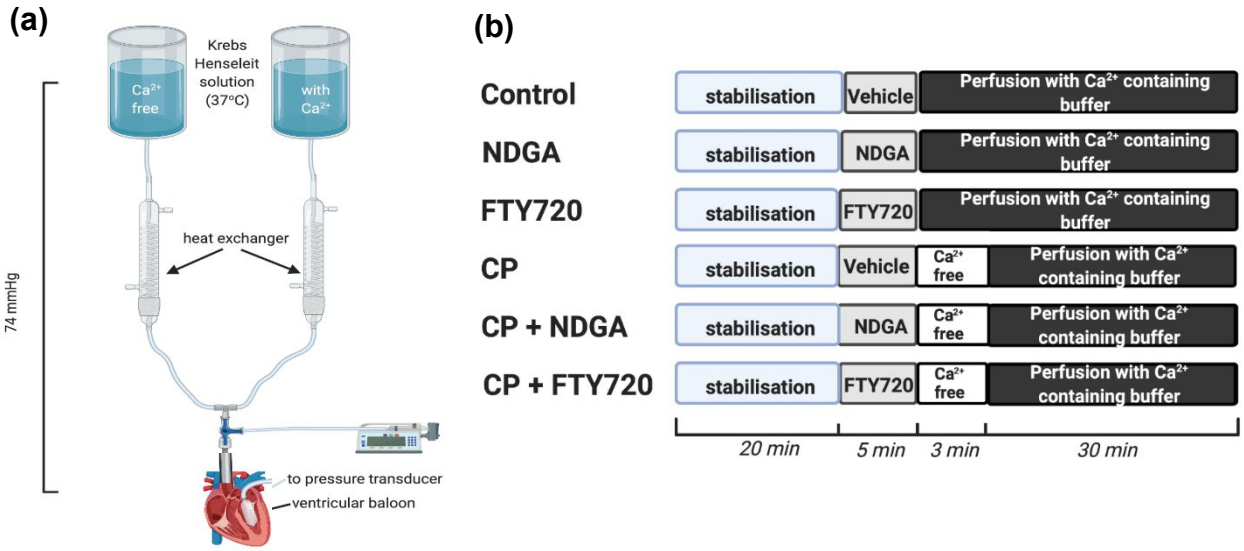

FIGURE 2.

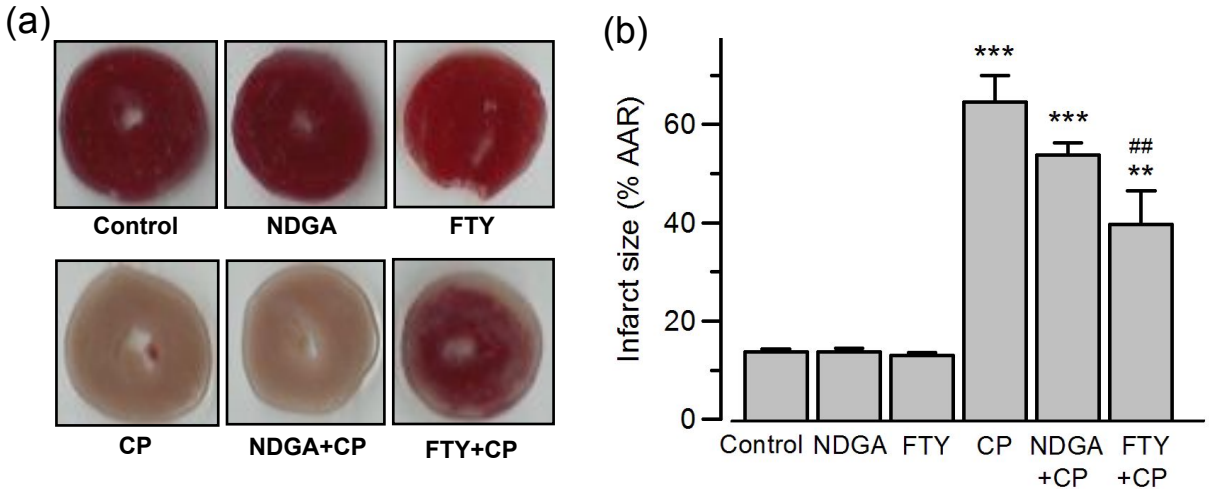

FIGURE 3.

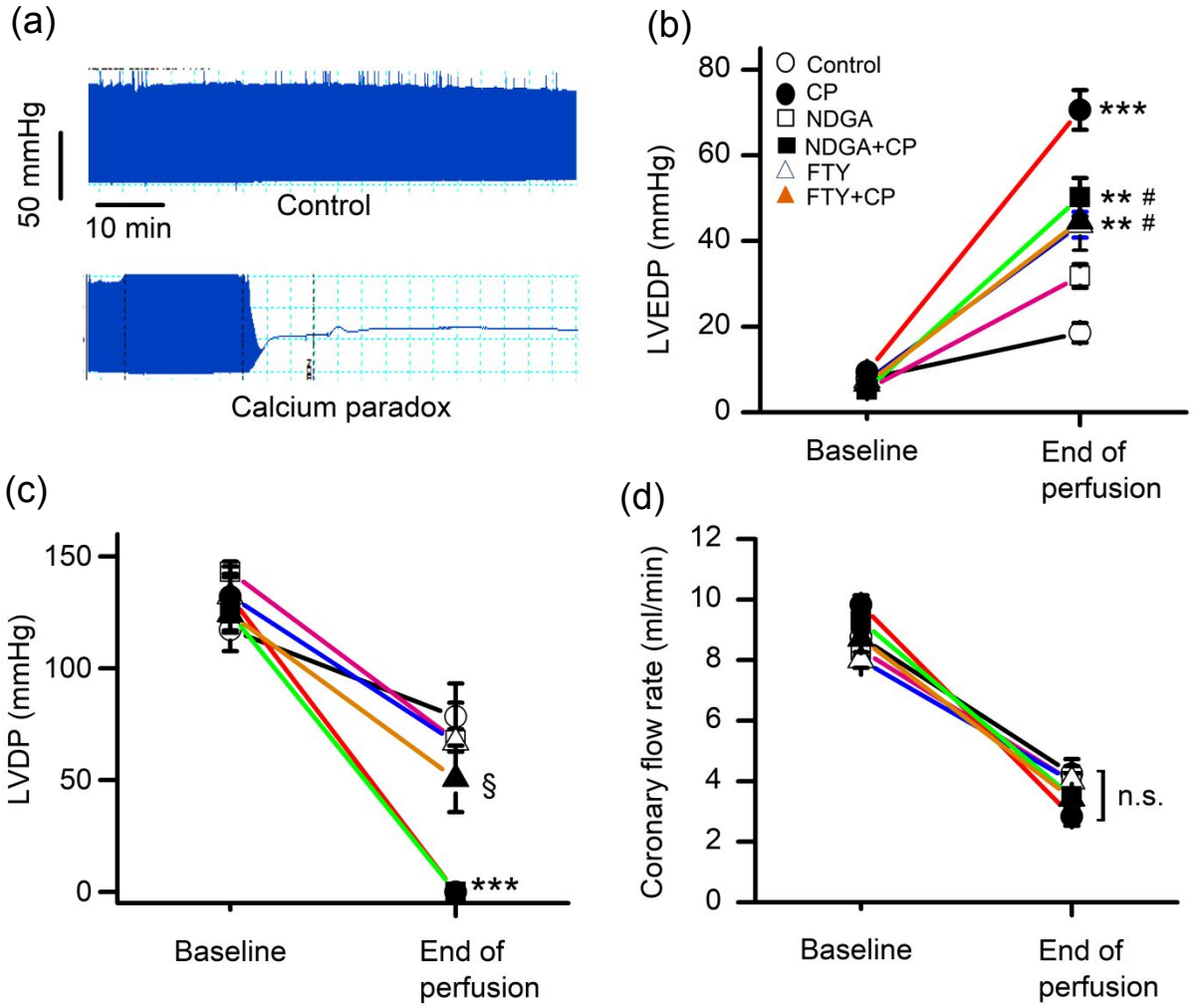

FIGURE 4.

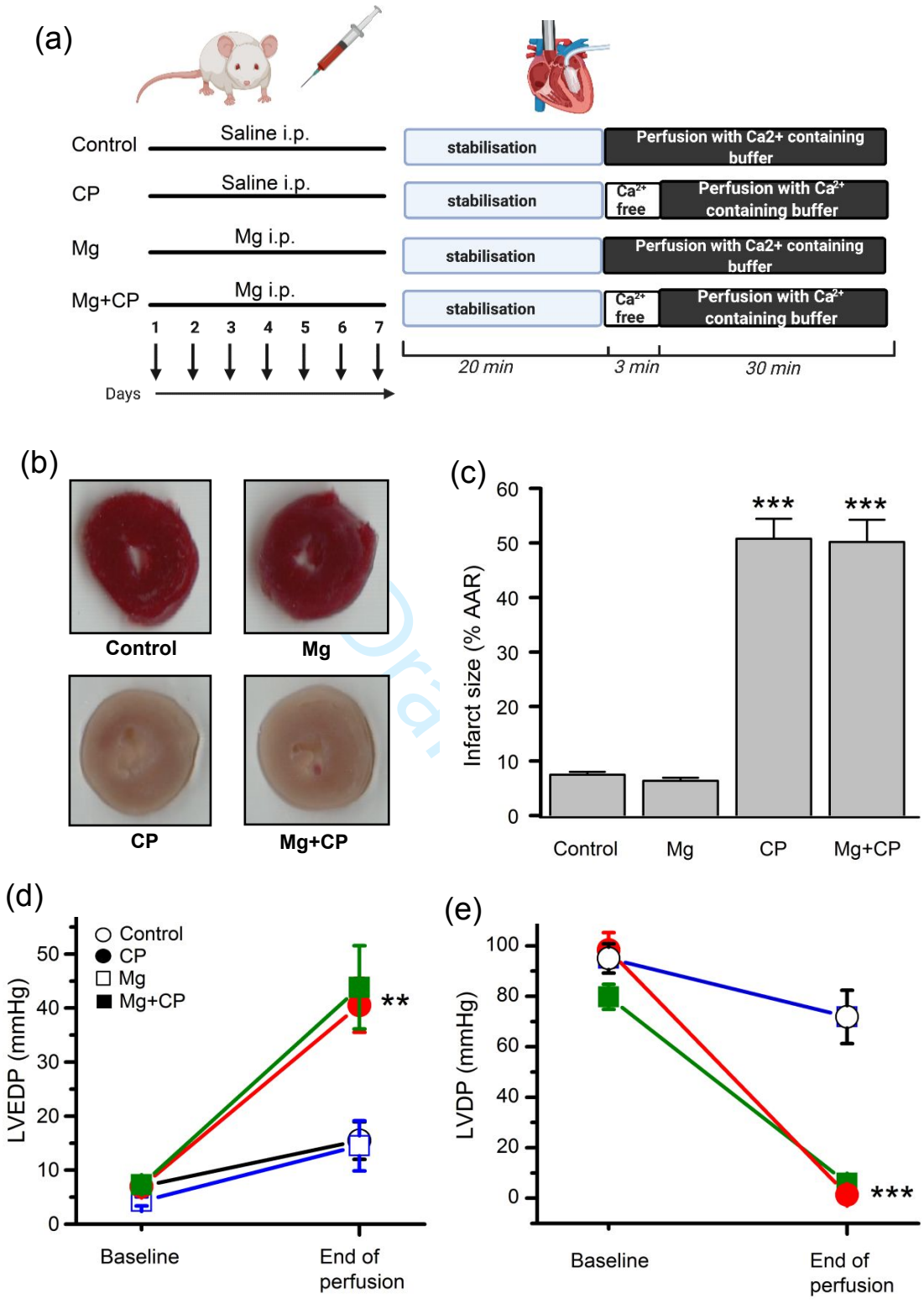

FIGURE. 5